

Investigation of Histotripsy Cavitation and Acoustic Droplet Vaporization From Perfluorocarbon Nanoparticles

Dylan Irie Pearson

Thesis submitted to the faculty of the
Virginia Polytechnic Institute and State University
in partial fulfillment of the requirements for the degree of

Master of Science
In
Biomedical Engineering

Eli Vlasisavljevich, Chair
Vincent M. Wang
Yasemin Durmaz

May 9, 2023
Blacksburg, Virginia

Keywords: Focused Ultrasound, Histotripsy, Nanoparticles, Nanoparticle-mediated Histotripsy

Copyright © 2023, Dylan Pearson

Investigation of Histotripsy Cavitation and Acoustic Droplet Vaporization From Perfluorocarbon Nanoparticles

Dylan Irie Pearson

ACADEMIC ABSTRACT

Histotripsy is a non-invasive and non-thermal focused ultrasound therapy that can be used to ablate tissue within the body while overcoming many of the limitations of thermal ablation. Histotripsy utilizes short-duration, high pressure ultrasound pulses to create a cavitation bubble cloud of numerous rapidly expanding and collapsing bubbles, which cause mechanical stress on the targeted region. Histotripsy contains multiple subtypes including intrinsic threshold, shock scattering, and boiling histotripsy, where intrinsic threshold histotripsy utilizes single cycle pulses focused to a single point to create a bubble cloud from the peak negative pressure ($p \geq 25$ MPa for water-based tissues). Nanoparticle-mediated histotripsy (NMH) uses perfluorocarbon-filled nanoparticles to create bubble clouds at lower pressures than that of the intrinsic threshold of histotripsy. Prior studies have shown that nanodroplets (NDs) and nanocone clusters (NCCs) both reduce the cavitation threshold, but further investigation on different parameters to optimize treatments have not fully been studied. Additional research is needed for the characterization of these nanoparticles with different pulsing parameters such as cycle number and frequency in order to better predict and understand the mechanisms underlying NMH.

In this thesis, I investigate the ability of new nanodroplets and nanocone clusters to reduce histotripsy cavitation threshold with NMH. I also investigate the effect that multi-cycle pulsing parameters have on NMH and stable bubble formation from acoustic droplet vaporization (ADV) for nancone clusters. The culmination of this thesis will advance our understanding of the behavior of acoustically-active nanoparticles when exposed to varied pulsing schemes and frequencies. This knowledge will allow for the further investigation of more efficient, effective, and safe methods for clinical focused ultrasound therapies.

Investigation of Histotripsy Cavitation and Acoustic Droplet Vaporization From Perfluorocarbon Nanoparticles

Dylan Irie Pearson

GENERAL AUDIENCE ABSTRACT

Histotripsy is a non-invasive and non-thermal focused ultrasound therapy that can be used to destroy targeted tissue within the body. Histotripsy is currently being developed for non-invasive and non-thermal cancerous tissue destruction with the first-in-man trial having been conducted within the last year for the treatment of liver tumors. Histotripsy utilizes high-pressure, short-duration pulses focused to a single region to create a cloud of bubbles that are rapidly expanding and collapsing which causes mechanical damage to the targeted cells. Nanoparticle-mediated histotripsy (NMH) has been developed to utilize nanoparticles to reduce the pressure needed to induce cavitation. Despite many studies and advances in histotripsy, there are many areas within the topic that need additional research to better understand the capabilities of the treatment method. This additional research is crucial in allowing for the development of new nanoparticles, faster treatment times, and new parameters that could allow for more precision near critical structures.

In this thesis, I investigate the ability of new nanoparticles to reduce histotripsy cavitation threshold with NMH. I also investigate the effect that multi-cycle pulsing parameters have on NMH and stable bubble formation for nanoparticles. The culmination of this thesis will advance our understanding of the behavior of acoustically-active nanoparticles when exposed to varied pulsing schemes and frequencies. This knowledge will allow for the further investigation of more efficient, effective, and safe methods for clinical focused ultrasound therapies.

Dedication

This is dedicated to my dog Bowser and my cat Guts, they will never know what a thesis is but they were a big help along the way.

Acknowledgements

I want to start by thanking Dr. Eli Vlasisavljevich for giving me a chance to join his incredible lab and providing me with all of the resources that I needed to grow as a researcher, collaborator, and person. You are definitely the most enthusiastic learner I may have ever seen and it spreads to everyone else around you. I went from having no idea how to even pronounce histotripsy to finding myself talking to other lab members or people in my life for sometimes hours at a time on different facets of bubbles. You have certainly fostered a strong, respectful, fun, and extremely collaborative environment with everyone in the lab and I always leave any meetings we have excited to learn more.

I want to also thank Dr. Vincent Wang and Dr. Yasemin Yuksel Durmaz for choosing to become members of my committee and offer their time, insight, and support throughout this entire process. You were never hesitant to provide me with feedback for any questions I may have asked at any time of day, and I would have had a much more arduous journey to get to this point without your help.

I absolutely have to thank Sarah Hall for everything that she has done and continues to do to support me. I try to thank her as much as I can but now that I'll have it in writing I can just set up a timed weekly email to send her this section for the next few years or so to get my point across. You have gone way above and beyond in your support for me, with the more that I progress in the process the further I am baffled on how you seemingly effortlessly continue to prove yourself to be an excellent role model and lab member in new ways each time. I have to also acknowledge Victor Lopez, Jess Gannon, Sara Elnahhas, Alex Simon, Lexi Stettinius, and anyone and everyone else that has been in the lab during my time here. You guys have all at some point been subjected to messages, emails, questions, or everything in between from me for help with tutorials, understanding a topic, learning to 3D print, learning to 3D design, setting up systems, finding papers, and too many other things to list. That's also one of the best parts about this lab is the fact that while you all have taken the time out of your days to walk me through how to set up or learn any of these things, you all also do not hesitate to do the same thing for each other and anyone else that may need help. The lab is an

incredibly collaborative little group and it would not be that way if not for the kind-heartedness and willingness to learn from each of you.

I want to thank my mom Pepsi, dad Bill, and sister Madison for supporting me my entire life to get this far. I am the one of the first members of my entire family to graduate college and the first member to reach graduate school, and that is entirely thanks to your constant help, love, advice, and support. There are too many things to express to fit into words here--so I won't! I will be telling you guys how great you are for many more years to come anyway. I have to also thank my grandfather Frank Jeffries who pretty much taught me how to read, count, do math, and always strive to be a kind person. Thanks to my grandma Peggy for always loving her grandkids with her whole heart and thanks to the rest of my family for all of the support as well.

To my girlfriend Makenna, thank you for the surprise gifts, Survivor watches, and endless love and cheers for both me and Guts. It makes things a lot easier to do when you have someone who is always believing in you no matter what, even in times when I might not be! Thanks to all of my other friends Andrew, Stephen, Bella, Craig, Diana and Ronnie, and a lot of others (I've been very lucky!) for helping me keep my sanity whether it be playing games, filming videos, trying new food, or watching Naruto every week for almost 2 years in a row. I now can empathize a bit with the actors at the Oscars who keep naming more and more people so that everyone gets recognition so I will end by casting a wide net and thanking everyone else who has ever helped me in life get to this place as both a student and a person. I'm excited to see what the future holds!

Dylan Pearson

May 2023

Table of Contents

Chapter 1: Introduction

1.1 Current State of Cancer Therapy Background	1
1.2 Histotripsy Ablation	2
1.3 Nanoparticle-mediated Histotripsy	3
1.4 Multi-cycle pulsing for NMH and ADV	6
1.5 Outline of Thesis	8

Chapter 2: Investigation of NMH Cavitation from Novel PEG Encapsulated Perfluorocarbon Nanodroplets

2.1 Background on Nanoparticle-Mediated Histotripsy	9
2.2 Previous Nanoparticles used for NMH	9
2.3 Methods: Investigating Cavitation Threshold for Nanodroplets	11
2.4 Results: Single-cycle NMH ND Study	14
2.5 Discussion	17
2.6 Conclusions	18

Chapter 3: Investigation of Acoustic Droplet Vaporization and Nanoparticle-Mediated Histotripsy Cavitation from PFH Nanocone Clusters

3.1 Introduction	20
3.2 Methods	22
3.3 Results: Cavitation Threshold Data of NCCs	27
3.4 Discussion: Multi-cycle Pulsing and NMH	30
3.5 Conclusions	31

Chapter 4: Conclusions and Future Work

4.1 Conclusions	33
4.2 Future Directions	33
References	34

Chapter 1. Introduction

1.1 Current State of Cancer Therapy Background

Since the inception of the COVID-19 pandemic, the world is focused more than ever on conversation regarding disease, disease prevention, and improved therapies. Cancer, in its many forms, has been one of the most formidable diseases throughout the years with new technologies, therapies, and treatments constantly being investigated and proposed to increase the quality of life for patients [1]. Many of the most widespread treatment methods involve surgical resection, radiation therapy, or chemotherapy [2,3]. These treatment methods have shown some success but remain associated with significant disease progression and recurrence for many cancer types [4]. The tumors targeted by these therapies can vary in size, shape, location, and behavior, which leads to a large amount of difficulty in treatments using these conventional approaches [3]. As medical technology progresses in the effort to combat cancer, the desire for non-invasive, targeted, and patient-specific procedures and therapies has progressed in a comparable fashion [5]. The innovation of non-invasive medical approaches for treating cancer has come hand in hand with improved image-guidance systems for accurate and real-time imaging of treatment [6]. Tumor ablation is one of the most commonly used treatments that is minimally invasive and results in the thermal or mechanical disruption of the cancerous tissue [7,8]. The most common ablation technologies are designed to combat tumor growth with techniques that utilize thermal energy to non-invasively induce cell death through either hyperthermia or cryoablation [5,9]. The most commonly used methods used for thermal ablation are radiofrequency, microwave, laser, and cryoablation [10–12]. Thermal ablation can also be applied non-invasively using high-intensity focused ultrasound (HIFU) pulses. HIFU is applied by a focused ultrasound transducer located outside the body that applies long-duration pulses (> 10 ms) to a targeted

tumor, resulting in the thermally-induced necrosis of the targeted tissue [13]. There has been an increased use of thermal ablation treatments within the past decade for applications such as the treatment of liver tumors and enlarged or cancerous prostates [9,14–16]. Thermal treatment methods have shown promise for ablating tumors < 3 cm in diameter in multiple cancers, but these methods also have limitations due to heat sink effects that cause variability in both treatment region size and ablation efficiency, particularly in highly vascular tumors [17]. HIFU can also be further limited by the heterogeneity and location of tumors within the body, long treatment times, and the reliance on expensive external imaging options such as magnetic resonance imaging (MRI) thermometry [14,18,19]. The prolonged exposure of high-intensity treatment has also been shown to cause damage such as burns to surrounding untargeted healthy tissue while attempting to perform ablation, leading to potentially unpredictable damage resulting from treatment [13,15,19]. Another holdback of thermal ablation methods is that due to the excessive treatment time, they are not suitable for treating multiple tumor nodules and are therefore not capable of treating most patients with late-stage metastatic cancers [10,14].

1.2 Histotripsy Ablation

Histotripsy is a non-invasive and non-thermal focused ultrasound therapy that can be used to ablate tissue within the body while overcoming many of the limitations of thermal ablation [7]. Histotripsy is currently being developed for non-invasive and non-thermal cancerous tissue ablation with two clinical trials having been conducted since 2020 [21,22]. The non-thermal properties of histotripsy are due to its short pulses which allow for the treatment of tumors near critical structures [7,23]. Histotripsy contains multiple subtypes including intrinsic threshold, shock scattering, and boiling histotripsy, where intrinsic threshold histotripsy utilizes single cycle pulses focused to a single point to create a bubble cloud from the peak negative

pressure ($p_- \geq 25$ MPa for water-based tissues) [23]. This bubble cloud is composed of many individual nanoscale nuclei that rapidly expand to form micron-sized bubbles which all rapidly collapse, causing mechanical damage to the surrounding cells during treatment [7,23]. The stress on the surrounding tissue has been shown to break down cancerous tissue into acellular debris while being closely monitored using real-time ultrasound imaging [8,23]. In terms of clinical applications, very high-pressure pulses used in histotripsy require very powerful transducers and can only be delivered to the targeted tumor effectively when the cancerous tumors can be properly imaged prior to and during treatment [8,18,24]. With many forms of cancer, patients are diagnosed at a late stage with multifocal or metastatic disease, making it difficult to effectively image and target every location of cancerous tissue within the body [25,26].

1.3 Nanoparticle-Mediated Histotripsy

Nanoparticle-mediated histotripsy (NMH) utilizes the precise non-invasive and non-thermal qualities of histotripsy combined with synthesized nanoparticles that are designed to reduce the cavitation threshold by a significant margin [24]. The cavitation threshold is defined as the peak negative pressure, p_- , where the probability of one or more bubbles nucleating during a pulse is equal to 50%, with NMH nanoparticles being capable of significantly reducing this threshold to approximately 10-15 MPa [7,18,23,24]. The first step in the NMH process is known as acoustic droplet vaporization (ADV) where the cores of the nanoparticles undergo a phase shift from liquid to gas after encountering an acoustic wave [27,28]. These acoustically-active nanoparticles are able to reduce the cavitation threshold by acting as the cavitation nuclei themselves [29]. The perfluorocarbon (PFC)-encapsulated nanoparticles act as histotripsy agents and are commonly composed of either perfluoropentane (PFP) or perfluorohexane (PFH) cores [18,19]. The PFC cores inside the nanoparticles have a lower nucleation threshold due to their

lower boiling points (29° and 56°C for PFP and PFH respectively) which enable them to both reduce cavitation threshold for histotripsy and form stable bubbles with ADV under the right conditions [28,30–32]. ADV can lead to either tumor embolization by using stable bubbles or transient cavitation as seen in NMH therapy depending on the parameters used [32–34].

The nanoparticles were first synthesized as nanodroplets (NDs), then later as nanocones (NCs), and most recently as nanocone clusters (NCCs) which all require chemical expertise to synthesize [24,29]. While the NDs were shown to reduce cavitation threshold during their original studies (~10-15 MPa from 25-30 MPa), the expertise required for their synthesis brought many challenges with the most prominent being the inability to know the amount of PFC within the core [24,30]. NCs were then designed to be the next generation of nanoparticles with cyclodextrin (CD) as a host molecule that holds PFC within its core to form a “nanocone” complex [29,30]. Previous studies have shown NCs to significantly reduce cavitation threshold reliably, but with the caveat that an optimal derivative of CD for histotripsy was not yet found due to variations in their solubility profiles and complex formation potential [24,29,30]. This led to the development of an improved histotripsy agent in NCCs which is the aggregation of some CDs and their derivatives with either PFH or PFP to increase solubility and stability while also being able to be stored for longer durations in the form of a powder [30,35]. Previous studies with NDs and NCCs have also shown selective cavitation within tissue-mimicking agarose gels, demonstrating the potential of using NMH as a targeted non-invasive treatment for multifocal or metastatic tumors in future clinical applications [24,32]. This is due to the reduced cavitation threshold of the nanoparticles that allow for targeted cavitation in regions containing the nucleating agent, which reduces the need for secondary imaging to guide treatment [31,36]. The most recent generation of nanoparticles used for this study alongside NCCs are newly

synthesized NDs that were formulated with the key difference from previous works in that we are able to use PEG500 to determine the PFH amount within the ND core. This means that for all current and future studies utilizing these NDs, the specific PFH amounts can be fine-tuned for each experiment. This can provide crucial data regarding PFH concentration's relationship to cavitation threshold and allow for more predictable NMH therapy delivery *in vivo*. These NDs can potentially be used for combination therapy such that the particles can dually function as cavitation agents and drug delivery vehicles.

Clinically, NMH nanoparticles would be injected into a patient and delivered to specifically targeted tumors. There are two primary mechanisms that enable these nanoparticles to localize in tumorous tissue, the enhanced permeability and retention (EPR) effect and the active targeting moieties attached to the outside of the nanoparticle [37]. The EPR effect is a phenomenon that involves the size of the invading nanoparticles and their ability to infiltrate tumor tissue [37]. This is helpful because of the role that size plays in immune response where larger foreign molecules are more quickly detected and engaged by the immune system than smaller molecules are [37,38]. Previous studies have extensively researched tumorous pathology to find that their vasculature is permeable to molecules of sizes smaller than approximately 200 nm in diameter [37,39,40]. A widely known hallmark of tumors is their ability to rapidly grow and replicate cells [3]. To stimulate this rapid growth and to provide nutrients to the continuously-growing tumor, the genesis of blood vessels at a rapid rate is required which leads to inefficient or abnormal structural features. These abnormalities are known as leaky vasculature and affect the fluid dynamics surrounding the tumor in ways that are not present in healthy regions of the body [41]. Molecules that are small enough to penetrate these structural gaps are then able to localize and be retained in tumorous tissue. An active mechanism within the

nanoparticles that is used alongside the EPR effect is the targeting peptide tags that localize to specific cancer cells, such as the use of EPPT1 peptide as a targeting ligand for receptors on the surface of breast cancer cells [42]. Finally, PEGylation is the final main method of active mechanisms that the nanoparticles use to travel into tumor vasculature. PEGylation is the attachment of polyethylene glycol (PEG) to the nanoparticles due to the immunogenicity suppressive effects of the polymer chains [43,44]. PEG is a hydrophilic coating that masks the nanoparticle when it is flowing through the bloodstream to slow or potentially stop recognition by the immune system [43,44]. The PEG polymer is non-toxic, non-immunogenic, and highly soluble in water and these qualities are exhibited by the nanoparticle in translation when it is coated in PEG to allow for more longevity in the bloodstream [43,44]. The combination of the NDs or NCCs potentially localizing near the tumorous tissue and their ability to cavitate at significantly lower pressures than histotripsy would allow for treatment to be conducted without the need for any real-time imaging [24,45]. Prior NMH studies have demonstrated the ability to successfully lower the cavitation threshold and ablate multiple cancer cell types including both prostate and breast cancer [46,47]. We hypothesize that the newly formulated NDs will reduce the cavitation threshold similar to the NCCs as demonstrated in previous NMH studies.

1.4 Multi-cycle Pulsing for NMH and ADV

While the histotripsy methods described thus far utilize single-cycle acoustic pulses, shock scattering histotripsy has also been found to be a viable method for cavitation cloud formation and tissue ablation with the use of multi-cycle parameters [48,49]. While intrinsic threshold histotripsy utilizes the negative pressure wave to trigger the rapid cavitation of a bubble cloud, shock scattering histotripsy uses multi-cycle (3-20) short-duration pulses to form a bubble cloud at a targeted area [48]. The increase in cycles causes the nuclei to undergo

cavitation and scatter shock waves to form a dense bubble cloud growing towards the direction of the transducer [48,50]. The compounding effect from the initial pressure release from the bubbles and the multiple shock fronts that are created from the multiple pulses allows for a much denser bubble cloud to be formed at a negative pressure lower than what is required for intrinsic threshold histotripsy [48,50]. Due to the nature of bubble cloud formation with shock scattering, it is typically used for the treatment of deep tumors to avoid the damage of healthy tissue with off-target effects [48]. As of yet, there have not been many published studies focusing on the benefits of multi-cycle pulsing relating to NMH. The differing cavitation dynamics from that of intrinsic threshold histotripsy may have a positive effect on reducing cavitation threshold further than previously studied for NMH, which could have additional benefits for the development of NMH therapies for a variety of cancer types and locations.

ADV and similar therapies have been used in drug delivery and the treatment of malignant neoplasms within the body via blood vessel occlusion [32,33,51]. With ADV being the vaporization process, utilizing an acoustic field via ultrasound can stimulate nanodroplets to the point where they vaporize into stable larger bubbles, which can wedge inside vascular structures and starve off cancerous tissue, or become inertial bubbles for NMH depending on parameters. Stable bubble formation has only been observed for micron-sized droplets whereas ADV only leads to transient cavitation when using nanoscale particles [38,52]. Similarly to shock scattering histotripsy, there have not been many published studies investigating the feasibility and benefits of inducing ADV with PFC NDs and NCCs. The potential for the same NDs and NCCs used for intrinsic threshold histotripsy to additionally be able to perform ADV and occlude blood vessels within tumor cells is a largely untouched avenue of potential therapies.

We hypothesize that NMH can be effectively applied using this histotripsy pulsing regime and that stable bubble formation following ADV will not occur due to the size of the nanoparticles.

1.5 Outline of Thesis

The goal of this thesis was to investigate the cavitation threshold of recently developed novel histotripsy nanoparticles and to characterize the cavitation effects when using both single and multi-cycle histotripsy treatments. In conjunction with the investigation of multi-cycle pulsing and its viability, the capability of using ADV with perfluorocarbon nanoparticles was also investigated. This thesis is broken into two primary chapters characterizing the NMH behavior of newly designed histotripsy nanodroplet formulations (Chapter 2) and investigating the effects of single and multi-cycle pulsing on NMH cavitation (Chapter 3). Finally, Chapter 4 summarizes and concludes the thesis, showcasing the general results from each study. Future work is then detailed and final comments on the next steps for NMH and multi-cycle pulsing as a viable treatment method are expressed.

Chapter 2. Investigation of NMH Cavitation from Novel PEG Encapsulated Perfluorocarbon Nanodroplets

2.1 Background on Nanoparticle-Mediated Histotripsy

Nanoparticle-mediated histotripsy (NMH) is a nonthermal, non-invasive focused ultrasound ablation therapy that utilizes exogenous cavitation nuclei, specifically perfluorocarbon (PFC)-filled nanoparticles, to reduce the cavitation threshold significantly compared to histotripsy (10 - 15 MPa) [24]. NMH causes mechanical disintegration of target tissue through the use of nanoparticles to seed acoustic cavitation when exposed to histotripsy (non-thermal focused ultrasound) pulses at pressures of ~8-12 MPa [24,45]. Clinically, these nanoparticles would be injected into a patient and delivered to specifically targeted tumors with the localization of nanoparticles to tumor tissue occurring due to PEGylation and the EPR effect [27,53]. A focused ultrasound pulsing scheme would enable the injected nanoparticles within the tumors to act as artificial cavitation nuclei to achieve targeted tumor cell ablation from the mechanical stress resulting from the rapid expansion and collapse of microbubbles.

2.2 Previous Nanoparticles Used for NMH

As illustrated in **Figure 2-1**, the nanoparticles are composed of a PFC core, most commonly either perfluoropentane (PFP) or perfluorohexane (PFH), forming polymer-encapsulated nanoparticles that are approximately 200-300 nm in diameter [53–55]. More recently, studies have developed alternative NMH nanoparticles in NCCs which are the aggregation of some CDs and their derivatives with either PFH or PFP to increase solubility and

stability while also being able to be stored for longer durations in the form of a powder [30,35]. Previous studies have identified PFH as being optimal for NMH applications when using both types of particles due to the fact that PFH-containing nanoparticles produced more compact and defined histotripsy bubble clouds [29,56].

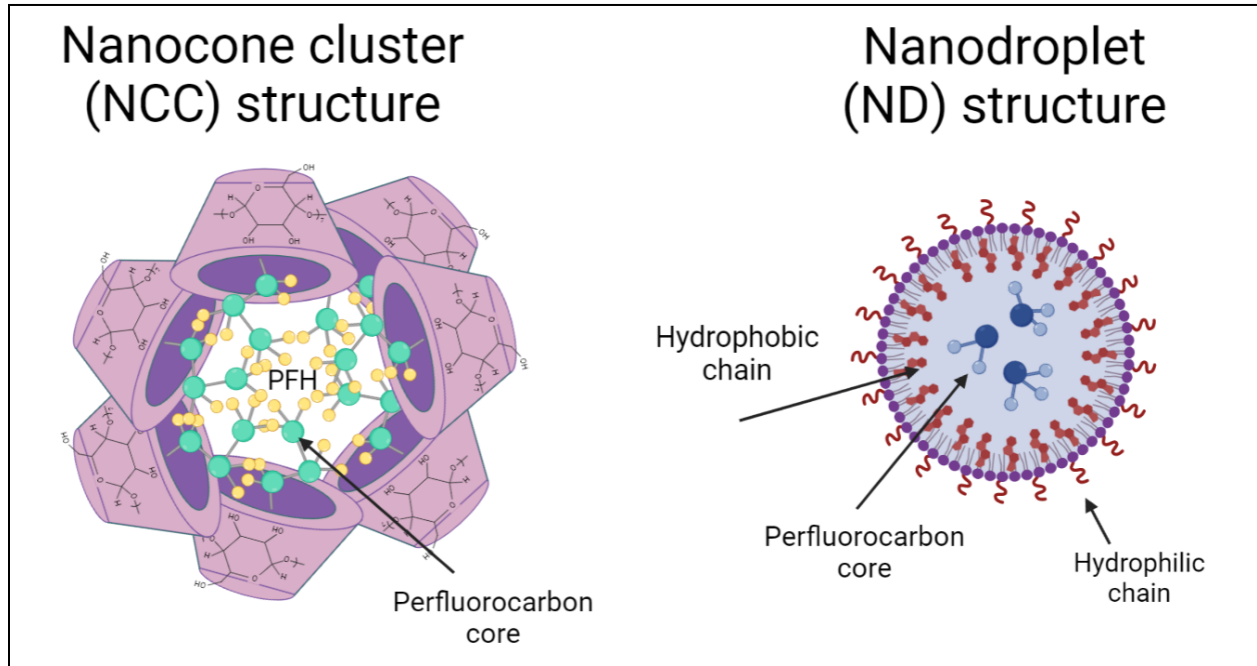


Figure 2-1. The components that comprise the perfluorocarbon nanodroplets and nanocone clusters. Nanodroplet structures are composed of PFP or PFH encapsulation. Nanocone cluster structures are composed of PFP or PFH encapsulated within a hydrophobic cavity of a cone-like hydrophilic structure.

The NDs and NCCs are synthesized by our collaborators from the Regenerative and Restorative Medicine Research Center at Istanbul Medipol University. Previous works have investigated the effects of an increase in PFC concentration on the ability to reduce cavitation threshold, showing the importance of the nanoparticle composition [24,57]. The cavitation threshold observed for each particle in previous studies has been shown to be similar for both types of particles (~10-15 MPa), ultimately depending on the type and amount of PFC present [29,30]. One limitation of

previously developed nanodroplets is the inability to precisely measure the PFC content within the core of the nanoparticle, which is essential for predicting NMH cavitation thresholds and determining the desired concentration of particles for delivering NMH.

2.3 Methods: Investigating Cavitation Threshold for Nanodroplets

2.3.1 Particle Synthesis and Gel Preparation

The nanodroplets are synthesized using self-assembly of a PEGylated fluoroalkyl polymer and PFH. The NDs were manufactured using PEGs of various molecular weights and fluoroalkyl polymers of different lengths to find the nanoparticle with the highest stability and efficiency. The composition of the NDs can be confirmed using GPC and the concentration of the PFH can be measured using gas chromatography.

Composition	Perfluorocarbon Core
PEG500-F5	PFH
PEG2000-F11	PFH
PEG500-F7	PFH
PEG500-F11	PFH
PEG2000-F7	PFH
PEG500-F9	PFH

Figure 2-2. Table listing the composition and core makeup of each ND tested for this study. Naming convention is the composition of the ND with PEGxxx being a PEG chain with mass xxx Da and Fx with x being the number of F groups in the fluoroalkyl chain.

2.3.2 Single-Cycle NMH Setup

For the experiments, some NDs were tested in tissue-mimicking agarose gel and some NDs were tested in liquid [58]. The gel was manufactured by mixing 1% agarose powder and 99% diluted PBS at room temperature until evenly dispersed. The diluted PBS was flash-boiled

until 50% of the volume remained to achieve a 1% degassed liquid agarose solution. The mixture was placed in a vacuum desiccator and kept under a partial vacuum for twenty minutes to remove any remaining gas. Once the temperature of the solution fell to 40° C, 100 mL of the mixture was added to a 3D-printed gel phantom holder. Immediately after this, ~10 mL of ND solution was added to the phantom holder and the entire solution was stored in a refrigerator for one hour to solidify.

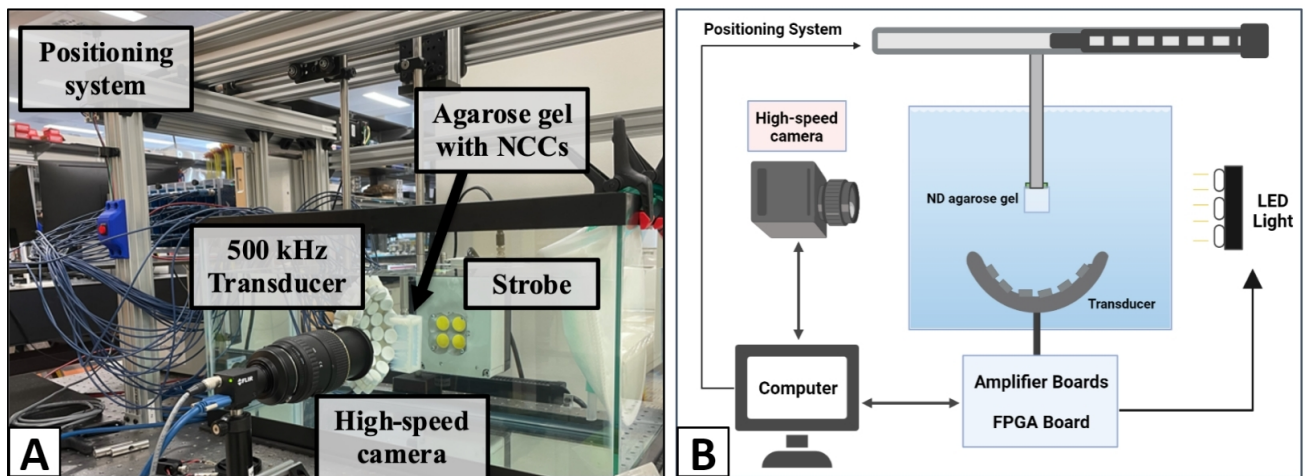


Figure 2-3. Images of the 500 kHz transducer and tissue-mimicking agarose gel setup (A) and a schematic of the components (B).

For NMH experiments in this study, a custom-built 500 kHz, 32-element transducer was used to deliver the single-cycle pulses as shown in **Figure 2-2**. Before threshold testing of the NDs, a tank was filled with water that was subsequently degassed for 2 hours to limit the amount of extraneous gas bubbles during experiments. The transducer was wired to interchangeable amplifier boards that populate a custom high-voltage amplifier. A field-programmable gate array (FPGA) board (Altera DE0-Nano Terasic Technology, Hsinchu, Taiwan) was programmed with a microcontroller to synchronize pulse arrivals when the system was running and was connected to send the driving signal to the amplifier boards. The FGPA board was connected to a power

supply, strobe, BlackFly high-speed camera (FLIR Blackfly S monochrome, BFS-U3-32S4M-C 3.2 MP, 118 FPS, Sony IMX252, Mono, FLIR Integrated Imaging Solutions, Richmond, BC, Canada), and desktop computer. The transducer was positioned parallel to the tank and perpendicular to the camera and strobe to ensure the most accurate capturing of the bubble cloud when images are taken. A MATLAB code was then run to initialize the system and provide an interface to freely alter parameters such as the pulse repetition frequency (PRF) or strobe brightness. The agarose gel was then attached to the positioning system over the tank containing the transducer and was lowered into view of the camera which was positioned in sight of the bubble cloud. The transducer was fired with a PRF = 0.5 Hz at 100 pulses with the camera shutter being electronically synced to the firing of each pulse. With the goal of the experiment being to characterize the cavitation threshold of the NDs in order to compare it to known pressure values without the presence of NDs, 100 images were captured for each pressure tested at slowly increasing pressures starting at 0 MPa and ending at 37 MPa. With cavitation occurring in water around the 25-30 MPa range, this testing range is sufficient to characterize the functionality of NDs as cavitation agents. A computer-guided 3D positioning system was controlled using MATLAB to orient the gel into focus using the live camera feed as a visual guide. The positioning system was used to move the gel in 3D in between each set of pulses to ensure that the transducer is not firing on a location that has been partially liquified after already being treated.

Liquid samples of NDs were then tested with the same transducer setup to allow for the highest concentration possible. The process for the preparation of the transducer, camera, and computer are all identical to that of the gel studies. For the liquid preparation, 1 mL of ND solution that was degassed in a vacuum desiccator for 24 hours was placed into a tube that was

connected to a holder and attached to the positioning system. The 1 mL of NDs were removed and replaced with a fresh sample in between each pressure tested.

2.3.3 Cavitation Threshold Calculation

Cavitation thresholds were obtained for each condition by determining the cavitation probability for each pressure level as the fraction of the total 100 pulses where cavitation was detected by optical imaging. MATLAB software was used for curve fitting for all data sets. The software was used by taking an image, binarizing it, counting the bubbles detected, and then calculating the probability using **Equation 2.1**. **Equation 2.1** gives the probability of observing cavitation following a sigmoid function to be

$$P(p_-) = \frac{1}{2} \left[1 + \operatorname{erf} \left(\frac{p_- - p_t}{\sqrt{2}\sigma} \right) \right] \quad (E2.1)$$

with erf being the error function, p_t being the negative pressure at which probability of cavitation is equal to 50%, and σ being related to the width of the transition between 0% cavitation and 100% cavitation [35,59].

2.4 Results: Single-cycle NMH ND Study

2.4.1 NMH Cavitation in Agarose Hydrogels

With the gel experiments, six different NDs were tested for their ability to act as cavitation agents. As shown in **Figure 2-4**, each ND was provided and tested at different concentrations. These variances are due to the synthesis process of the NDs, and with the intention to test as high of a concentration as possible for initial feasibility studies to characterize the respective cavitation threshold and resulting histotripsy bubble cloud behavior. All six NDs were shown to lower the cavitation threshold, but not to the desired range of 10-15 MPa. PEG500-F5 and PEG500-F11 lowered the threshold more than the other NDs with cavitation appearing at approximately 21.3 MPa as opposed to 25-27 MPa for the other particles. **Figure**

2-5 illustrates the probability of cavitation as a function of p_- for each of the droplet conditions, demonstrating the largest decreases in the cavitation threshold for PEG500-F11 and PEG500-F5. The x-axis is the peak negative pressure in MPa and the y-axis is the probability of cavitation. The pressure at which cavitation is first introduced for each ND is listed as p_- and σ is the standard deviation for each cavitation threshold.

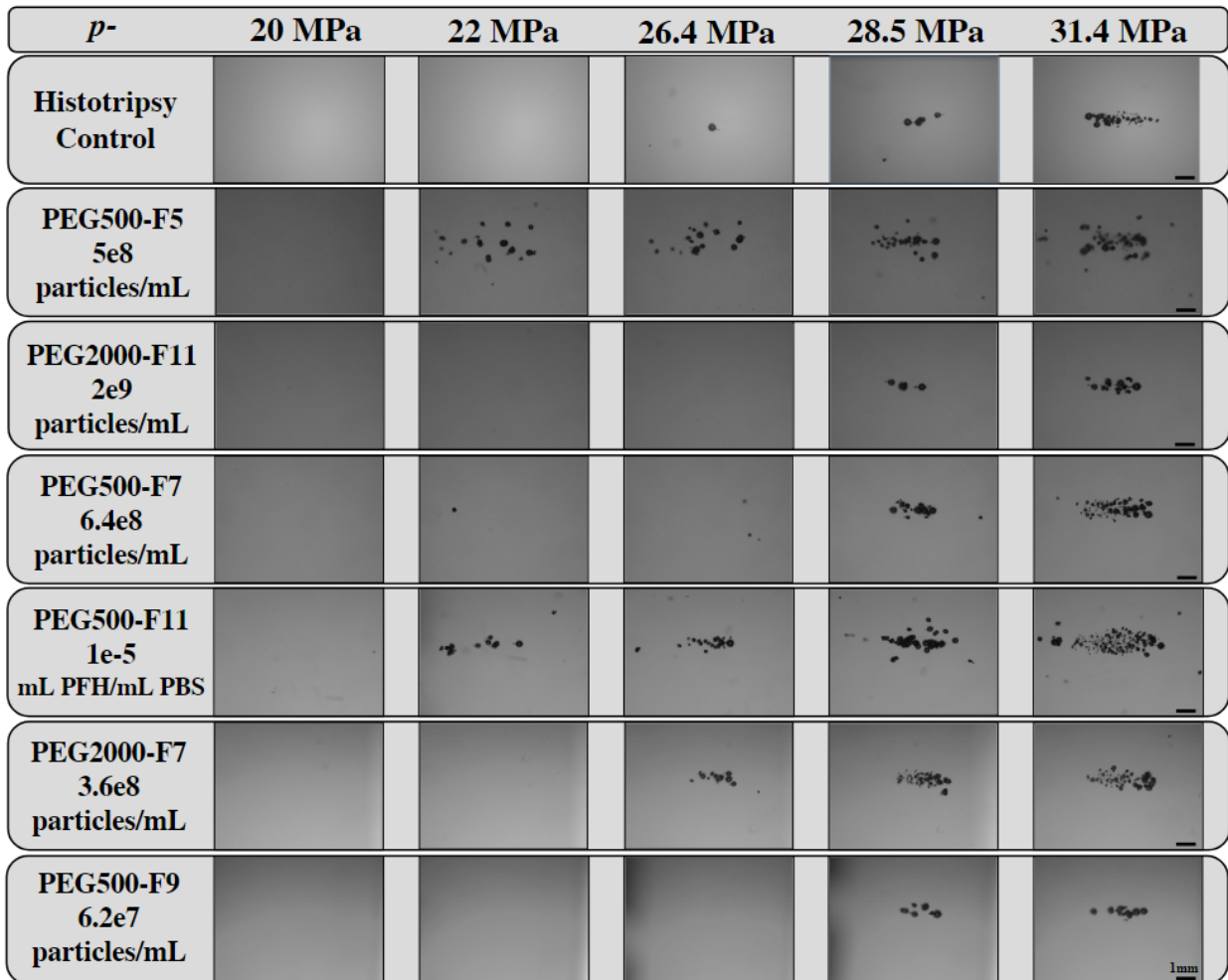


Figure 2-4. Images taken with BlackFly high-speed camera of bubble clouds within ND agarose gel at varying pressures. Each row is a different ND with its respective concentration listed in the left column. Top row is a control with no NDs present.

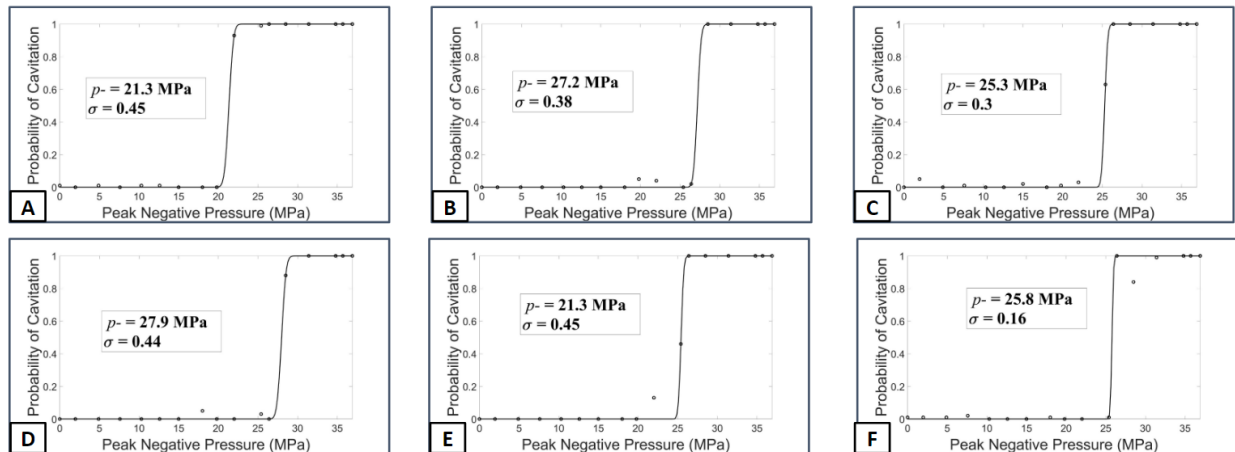


Figure 2-5. Cavitation threshold figures for each ND tested with the agarose gel studies. Histotripsy control threshold is ~ 26 MPa for reference. (A) PEG500-F5 PFH ND tested at 5×10^8 particles/mL. (B) PEG500-F7 PFH ND tested at 6.4×10^8 particles/mL. (C) PEG2000-F7 PFH ND tested at 3.6×10^8 particles/mL. (D) PEG2000-F11 PFH ND tested at 2×10^9 particles/mL. (E) PEG500-F11 PFH ND tested at 10^{-5} mL PFH/mL PBS. (F) PEG500-F9 PFH ND tested at 6.2×10^7 particles/mL.

2.4.2 NMH Cavitation in Suspension

PEG500-F5 was the ND used for the liquid studies due to the fact that it performed the best as a cavitation agent from the gel experiments. As shown in **Figure 2-6**, the cavitation threshold for PEG500-F5 with the liquid studies did not deviate from the testing in gel. This indicates that the gel studies for PEG500-F5 did not suffer a loss of concentration due to leakage or other human error and that the PFH content itself may need to be changed during ND synthesis.

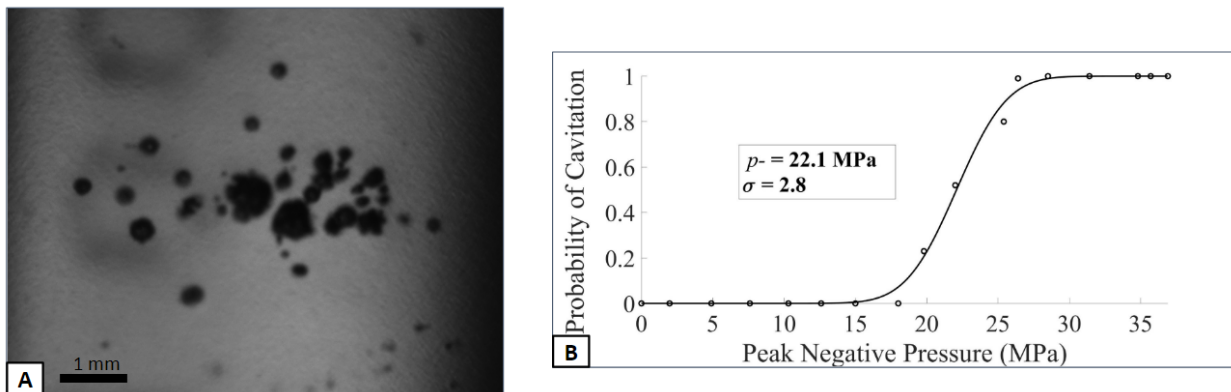


Figure 2-6. Image of cavitation bubble cloud at ~35 MPa (left) and data analysis of cavitation threshold (right). X-axis is the peak negative pressure in MPa and the y-axis is the probability of cavitation. p^- is listed for each ND and represents the pressure at which cavitation is first induced. σ is the standard deviation for each cavitation threshold.

2.5 Discussion

NMH has been shown to reduce cavitation threshold to pressures significantly lower than that of conventional histotripsy procedures due to the use of PFC nanoparticles [24,57]. The newly synthesized NDs developed and tested in this study have the unique ability to fine-tune PFH concentration within the core which has been shown in previous studies to affect the ND's ability to act as a cavitation agent. Experiments with these NDs in both tissue-mimicking gels and pure liquid form suggest that these NDs are feasible to be used as histotripsy cavitation agents. For each experiment with each formulation of NDs at varying conditions, the cavitation threshold was lowered compared to histotripsy, albeit not as substantially as previously studied NDs. Specifically for PEG500-F11, the manufacturers were able to inform us of the PFH concentration within the core which allowed us to use a concentration that could be used to compare to the previously mentioned studies of NCCs where the same concentration reduced the threshold. The lowered histotripsy cavitation threshold of these NDs shows that they are effective when used for NMH, which indicates that they could lead to potential developments for therapies. These NDs, once further optimized, can help to remove the need for larger and more

powerful transducers for histotripsy treatments due to the lowered pressure threshold that is required for cavitation. In order to acquire new NDs that lower the cavitation threshold to the desired range of 10-15 MPa, more repeated experiments on higher concentrations should be considered. As previously stated, the potential error in precise concentration values led to the testing of liquid NDs to allow for as high of a concentration as possible. With the data showing that the liquid study is comparable in threshold analysis to gel studies, these liquid studies should be considered as initial tests for NDs to pinpoint the most effective PFH concentrations and droplet formulations before moving to additional gel studies to simulate their capabilities when within a tissue-like substance. Ongoing studies are trying to refine the concentration of the PFC cores to lower the cavitation threshold and fully characterize the NDs based on stability and efficiency. For example, as shown in **Figure 2-7**, testing PEG500-F5 at 1.38×10^9 particles/mL and PEG500-F7 at 4.94×10^8 particles/mL lowered the threshold from ~ 22 - 25 MPa to ~ 11 MPa.

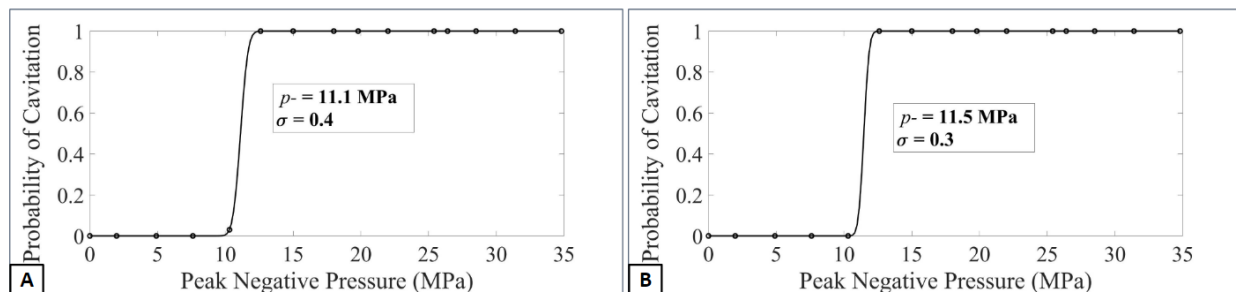


Figure 2-7. (A) Cavitation threshold curve for PEG500-F5 (B) Cavitation threshold curve for PEG500-F7. X-axis is the peak negative pressure in MPa and the y-axis is the probability of cavitation. ρ is listed for each ND and represents the pressure at which cavitation is first induced. σ is the standard deviation for each cavitation threshold.

2.6 Conclusions

Continuing from the findings of previous studies, new NDs were developed and tested to investigate their ability to act as histotripsy cavitation agents. The NDs reduced the histotripsy cavitation threshold to ~ 20 - 25 MPa from ~ 25 - 30 MPa which showed that they are effective for

use with NMH. Current ongoing studies have refined the concentration further to reduce the cavitation threshold to ~11 MPa for some NDs. Further studies will be needed to optimize these new particle formulations and concentrations for effective NMH therapy.

Chapter 3. Investigation of Acoustic Droplet Vaporization and Nanoparticle-Mediated Histotripsy Cavitation from PFH Nanocone Clusters

3.1 Introduction

Nanoparticle-mediated histotripsy (NMH) is a nonthermal, non-invasive focused ultrasound ablation therapy that utilizes exogenous cavitation nuclei, specifically perfluorocarbon (PFC)-filled nanoparticles, to reduce the cavitation threshold significantly compared to histotripsy (10 - 15 MPa) [24]. NMH causes mechanical disintegration of target tissue through the use of nanoparticles to seed acoustic cavitation when exposed to histotripsy (non-thermal focused ultrasound) pulses at pressures of ~8-12 MPa [24,45]. Clinically, these nanoparticles would be injected into a patient and delivered to specifically targeted tumors with the localization of nanoparticles to tumor tissue occurring due to PEGylation and the EPR effect [27,53]. A focused ultrasound pulsing scheme would enable the injected nanoparticles within the tumors to act as artificial cavitation nuclei to achieve targeted tumor cell ablation from the mechanical stress resulting from the rapid expansion and collapse of microbubbles.

Previous studies have investigated different pulsing parameters for NMH such as the effect of frequency and the effects of positive and negative pressure on NMH cavitation. Previous work investigating frequency has found that on multiple ultrasound frequencies (345 kHz, 500 kHz, 1.5 MHz, and 3MHz) the cavitation threshold was decreased [60]. Results in these studies showed that a lower frequency will improve the effectiveness of NMH by means of increasing the focal region size [60]. Studies on positive and negative pressure with NMH

investigated the physical mechanisms that caused the nanodroplet cavitation process [61]. Results from these studies provided insight into how negative pressure causes cavitation nucleation when the PFC core is exposed to it [61]. These studies among a few others have provided new insights into NMH but have typically relied on single-cycle pulsing.

The first step in the NMH process is known as acoustic droplet vaporization (ADV) where the cores of the nanoparticles undergo a phase shift from liquid to gas after being hit by an acoustic wave [27,28]. ADV and similar therapies have been used in drug delivery and the treatment of malignant neoplasms within the body via blood vessel occlusion [32,33,51]. With ADV being the vaporization process, utilizing an acoustic field via ultrasound can stimulate nanodroplets to the point where they vaporize into stable larger bubbles, which can wedge inside vascular structures and starve off cancerous tissue, or become inertial bubbles for NMH depending on parameters. Stable bubble formation has only been observed for larger droplets whereas ADV only leads to transient cavitation when using nanoscale particles [38,52,62]. Previous studies have investigated the use of ADV to produce stable bubbles at a high PRF (~100 Hz) and cycles typically ranging between 8 and 15 [33,38,62].

The investigation of the PFC nanoparticles as cavitation agents for this experiment focuses on shock scattering histotripsy, as opposed to the single-cycle intrinsic threshold method used in Chapter 2. With intrinsic threshold histotripsy firing a large peak negative pressure single pulse, shock scattering fires multiple cycles of pulses to induce and sustain cavitation [48]. This alteration of pulsing schematics, while both still lead to bubble clouds, create differing dynamics of cavitation. Previous work has examined the effects between intrinsic threshold and shock scattering histotripsy to show that treatment times can be significantly reduced with a higher PRF [48,63]. This is due to the time between pulses becoming much shorter with higher PRFs

compared to lower PRFs [31]. While investigating multi-cycle pulsing on NMH cavitation, these experiments will also investigate bubble dynamics including stable bubbles formed from ADV when using previously successful parameters at the nanoscale.

3.2 Methods

3.2.1 Particle Synthesis and Gel Preparation

For both the single-cycle and multi-cycle experiments, a 2% agarose gel was used due to its physical composition closely resembling that of tissue. The gel was composed using 150 mL of 1x PBS, 150 mL of deionized water, 3 g agarose, and a dissolved NCC solution. The NCCs were diluted in 55 mL PBS to a concentration of 1×10^{-5} mL PFH/mL PBS. The 300 mL of PBS and water was flash boiled to approximately 150 mL to achieve the 2% agarose solution and was then combined with the NCCs and cooled until a solid gel was formed. The combination of the solution and the NCCs resulted in a 1% agarose gel. The gel was then placed in a phantom holder and attached to the positioning system over the tank containing the transducer and was lowered into view of the camera that is positioned in sight of the bubble cloud.

3.2.2 Single-Cycle NCC Experiments

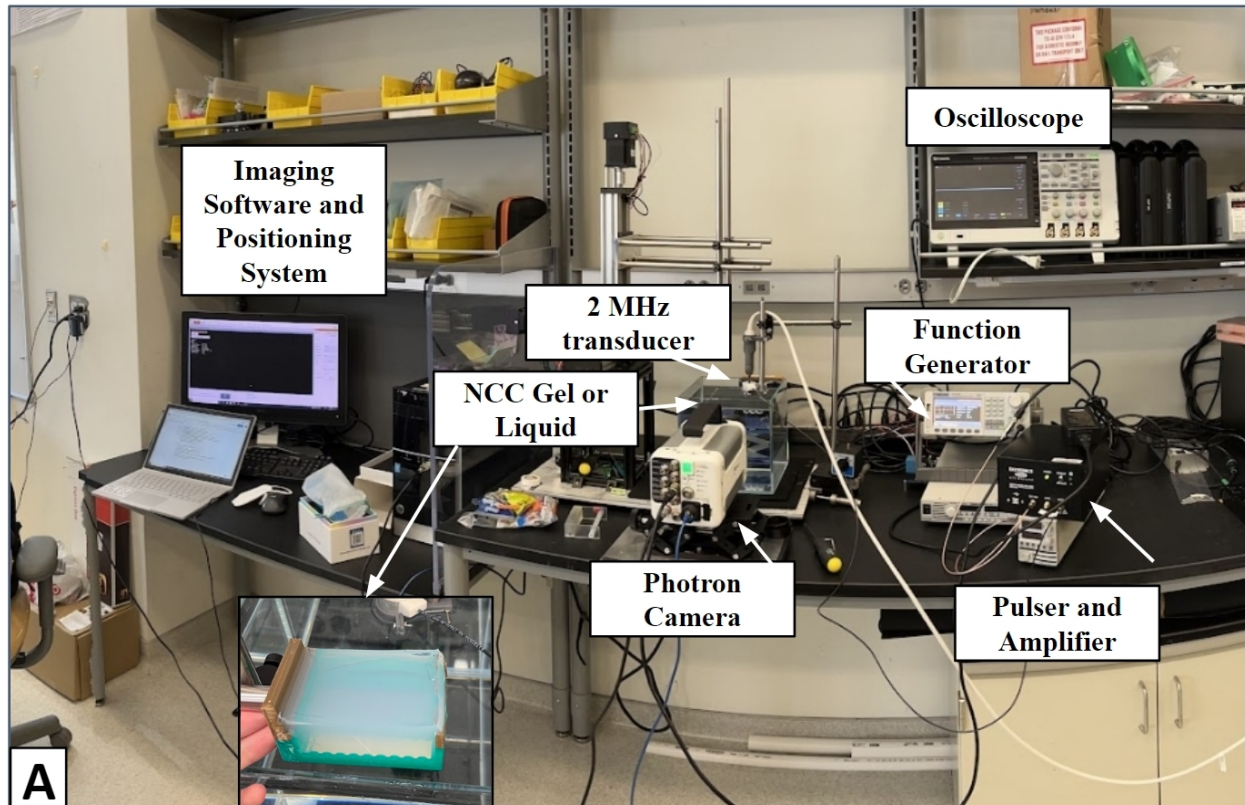
For NMH experiments in this study, a custom-built 500 kHz, 32-element transducer was used to deliver the single-cycle pulses as shown in **Figure 2-2**. Before threshold testing of the NDs, a tank was filled with water that was subsequently degassed for 2 hours to limit the amount of extraneous gas bubbles during experiments. The transducer was wired to interchangeable amplifier boards that populate a custom high-voltage amplifier. A field-programmable gate array (FPGA) board (Altera DE0-Nano Terasic Technology, Hsinchu, Taiwan) was programmed with a microcontroller to synchronize pulse arrivals when the system was running and was connected to send the driving signal to the amplifier boards. The FGPA board was connected to a power

supply, strobe, BlackFly high-speed camera (FLIR Blackfly S monochrome, BFS-U3-32S4M-C 3.2 MP, 118 FPS, Sony IMX252, Mono, FLIR Integrated Imaging Solutions, Richmond, BC, Canada), and desktop computer. The transducer was positioned parallel to the tank and perpendicular to the camera and strobe to ensure the most accurate capturing of the bubble cloud when images are taken. A MATLAB code was then run to initialize the system and provide an interface to freely alter parameters such as the pulse repetition frequency (PRF) or strobe brightness. The agarose gel was then attached to an optical rod over the tank containing the transducer and was lowered into view of the camera which was positioned in sight of the bubble cloud. The transducer was fired with a PRF = 0.5 Hz and PRF = 100 Hz at 100 pulses with the camera shutter being electronically synced to the firing of each pulse. With the goal of the experiment being to characterize the cavitation threshold of the NCCs in order to compare it to known pressure values without the presence of NCCs, 100 images were captured for each pressure tested over the range of 0 MPa to 37 MPa. With cavitation occurring in water around the 25-30 MPa range, this testing range is sufficient to characterize the functionality of NCCs as cavitation agents. A computer-guided 3D positioning system was controlled using MATLAB to orient the gel into focus using the live camera feed as a visual guide. The positioning system was used to move the gel in 3D in between each set of pulses to ensure that the transducer is not firing on a location that has been partially liquified after already being treated.

3.2.3 Multi-Cycle NCC Experiments

There have been previous studies utilizing NMH for single-cycle pulsing, but none using multi-cycle pulsing. As shown previously, NCCs were developed to address potential issues that came with NDs such as a smaller size or more readily detectable PFC amounts [24]. Every NCC tested with histotripsy for this document was composed of a PFH core. We hypothesized that

NMH will still be successfully capable of being generated from NCCs when using multi-cycle pulses, and designed an experiment to investigate further. Our secondary hypothesis is that stable ADV bubbles will not be generated due to the size of the nanoparticles. Many previous studies conducted on ADV investigated particles in the micron-size range, whereas the NCCs are much smaller in the nanometer range [27,28,32–34].



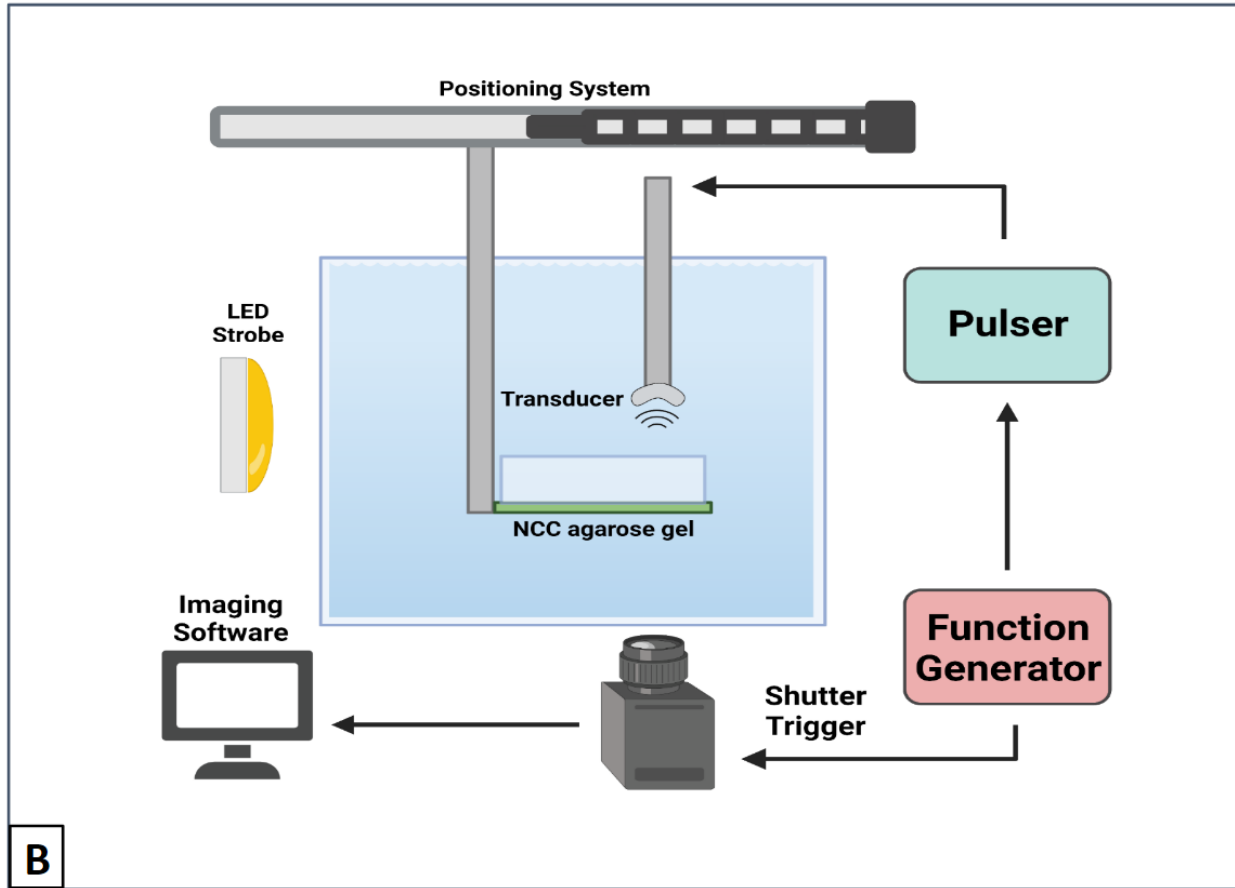


Figure 3-1. The setup for the multi-cycle experiments. (A) The full view of the entire setup with each component labeled and an insert image of a close view of the tissue mimicking gel. (B) High level schematic depiction of the process shown in (A).

For the NMH NCCs multi-cycle experiment, a 2 MHz transducer (Daxsonics) was used due to its ability to utilize a multi-cycle pulsing scheme. The transducer was calibrated at 12 cycles using an Onda Hydrophone and fiber optic hydrophone to accurately convert between input voltage and output pressure. The equipment setup consisted of the 2 MHz transducer, a function generator, an oscilloscope, a Nova S12 Photron camera, an amplifier, a strobe, a computer-guided 3-D positioning system, Daxsonics pulser, gel and liquid holders, and a small water tank. The parameters were set in the function generator with channel 1 having a frequency of 2 MHz and desired cycles with burst period set to on. **Figure 3-1A** shows the full setup when running, where the output of channel 2 was attached with a BNC cable to the TRIG TTL IN port

on the photron camera. In the function generator, a delay was set to correspond to a trigger after the final pulse in the 12-cycle scheme from channel 1 had been completed. This channel 2 signal was sent to the camera to prepare it to snap another image. The cycle of pulse, image, pulse, and image was repeated and was perfectly timed to be in sync with one another so that the full bubble cloud could be imaged. Secondary images were set to be taken in between pulses to ensure that each bubble was in fact newly cavitating and not a formed stable bubble due to ADV. Once the camera delay trigger was properly set, the transducer was attached to the Daxsonics pulser which in turn was connected to the output of channel 1 on the function generator. An amplifier was then connected to the pulser to determine the voltage at which the transducer was being fired. This caused a chain of events where the function generator set the pulses and timed the camera to accurately image them, these parameters were then fed into the Daxsonics system which then fed this information to the actual transducer which fired at the voltage set on the amplifier. This workflow allowed for multi-cycle pulsing at a changeable voltage with constant live imaging for monitoring. As for the NCCs, they were placed in an agarose gel created with the same recipe as the ND gel in Chapter 2. The key difference between preparing the NDs and NCCs was the need to dilute the NCCs in solution prior to placing them within the gel due to the fact that they were stored as a vacuum-dried powder as opposed to the ND's liquid form. The gel was then mounted on an optical rod that was connected to the computer-guided 3D positioning system and lowered beneath the 8 mm focal range of the transducer. An open water test was performed to both ensure that the transducer was firing properly and to locate the bubble cloud with the camera. Once this was completed, the gel was raised to be in view of the camera and the transducer was fired at increasing voltages. Histotripsy occurs in open water with these parameters at approximately 24 MPa, which informs the investigation of the cavitation threshold on the gel to be from 0-27 MPa

in increments of approximately 2 MPa. At every interval, 100 images were collected and then saved to an external hard drive. Upon completing the experiment, each trial was examined using MATLAB with the same parameters of previous studies of cavitation being deemed for an interval if at least 50% of the images contain a unique bubble.

3.2.4 Cavitation Threshold Calculation

Cavitation thresholds were obtained for each condition by determining the cavitation probability for each pressure level as the fraction of the total 100 pulses where cavitation was detected by optical imaging. MATLAB software was used for curve fitting for all data sets. The software was used by taking an image, binarizing it, counting the bubbles detected, and then calculating the probability using **Equation 2.1**. **Equation 2.1** gives the probability of observing cavitation following a sigmoid function to be with erf being the error function, p_t being the negative pressure at which probability of cavitation is equal to 50%, and σ being related to the width of the transition between 0% cavitation and 100% cavitation [35,59].

3.3 Results: Cavitation Threshold Data of NCCs

With the single-cycle experiments, the NCC was tested with a PRF of 0.5 Hz and 100 Hz. The 0.5 Hz PRF was tested both to reduce the memory effect and because it is the parameter that has been used in the previous experiments for characterizing nanoparticles as histotripsy cavitation agents, so it would provide an accurate value for the threshold. The 100 Hz PRF was tested because it is the parameter that was used for the multi-cycle experiments and would allow for comparison between this experiment and the multi-cycle experiments with the same NCC. As shown in **Figure 3-2**, the NCC successfully lowered the cavitation threshold to approximately 10 MPa compared to the approximately 19 MPa of the control. Additionally, the bubble cloud was visually much less dense and more peripheral bubbles were observed for the higher PRF

compared to the PRF of 0.5 Hz. **Figure 3-3** illustrates the probability of cavitation as a function of p_- for each of the NCC conditions, demonstrating the largest decrease in cavitation threshold for the NCC at the highest PRF. The x-axis is the peak negative pressure in MPa and the y-axis is the probability of cavitation. The pressure at which cavitation is first introduced for each ND is listed as p_- and σ is the standard deviation for each cavitation threshold.

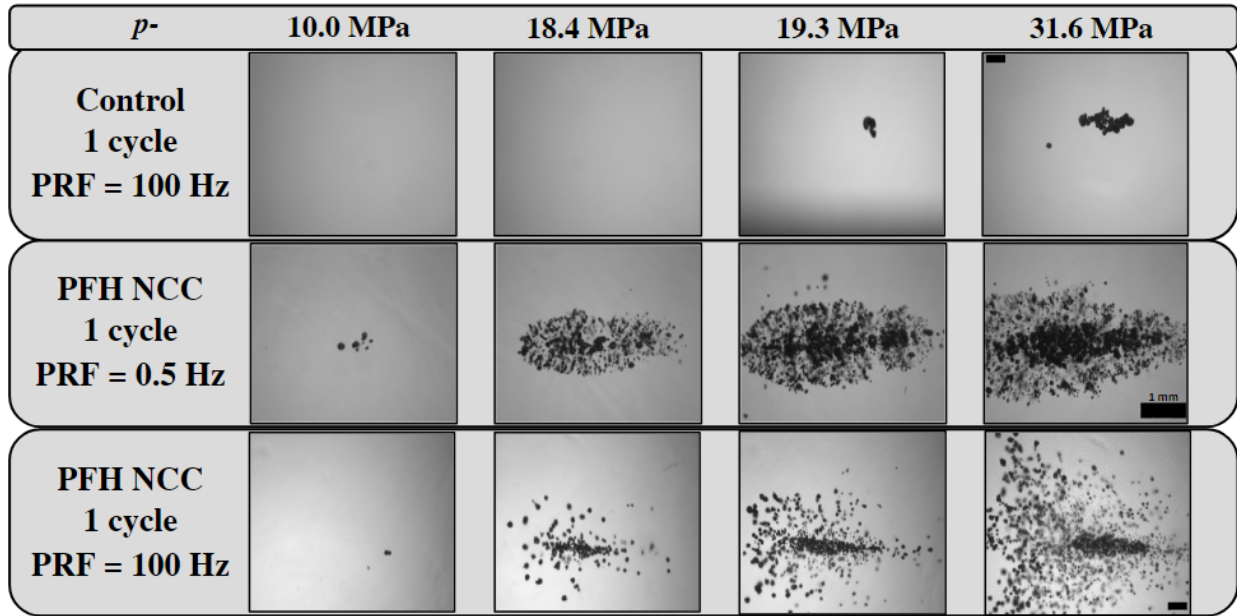


Figure 3-2. Images of cavitation bubble clouds for NCC gels under single-cycle pulsing schemes at varying PRFs using a 500 kHz transducer. As expected, the cavitation threshold was lowered with the use of NCCs for both of the PRFs tested.

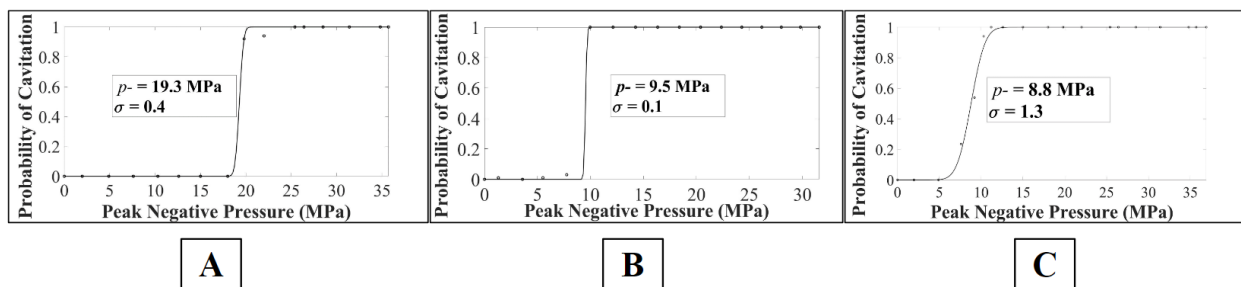


Figure 3-3. Cavitation threshold figures for single-cycle NCC experiments. (A) Control at 100 Hz PRF. (B) NCC at 0.5 Hz PRF. (C) NCC at 100 Hz PRF.

For the multi-cycle experiments, the NCC was tested at a PRF = 100 Hz at 5, 8, and 12 cycles. A control was tested only using 12 cycles at a PRF = 100 Hz since there is a negligible difference for multi-cycle thresholds above 3 cycles. As shown in **Figure 3-4**, for all multi-cycle variations the cavitation threshold was lowered from ~24 MPa to ~4.5 MPa. **Figure 3-4** also illustrates the probability of cavitation as a function of p - for each of the cycle variations, demonstrating the similarity in histotripsy cavitation threshold between the 5, 8, and 12 cycles. The p represents the pressure in MPa at which the cavitation threshold occurs for the NCCs. The σ is the standard deviation of pressure for the trial. As shown in the graphs, the cavitation threshold was lowered to expected values compared to that of the control. Other works conducted on NCCs using single-cycle pulsing have achieved the same results, indicating further that multi-cycle pulsing is a viable method for NMH. Frames were captured between pulses during the multi-cycle experiments to determine if there was any stable bubble formation following ADV. Each frame captured between pulses displayed no bubbles, showing that no stable bubble formation occurred during any of the multi-cycle testing.

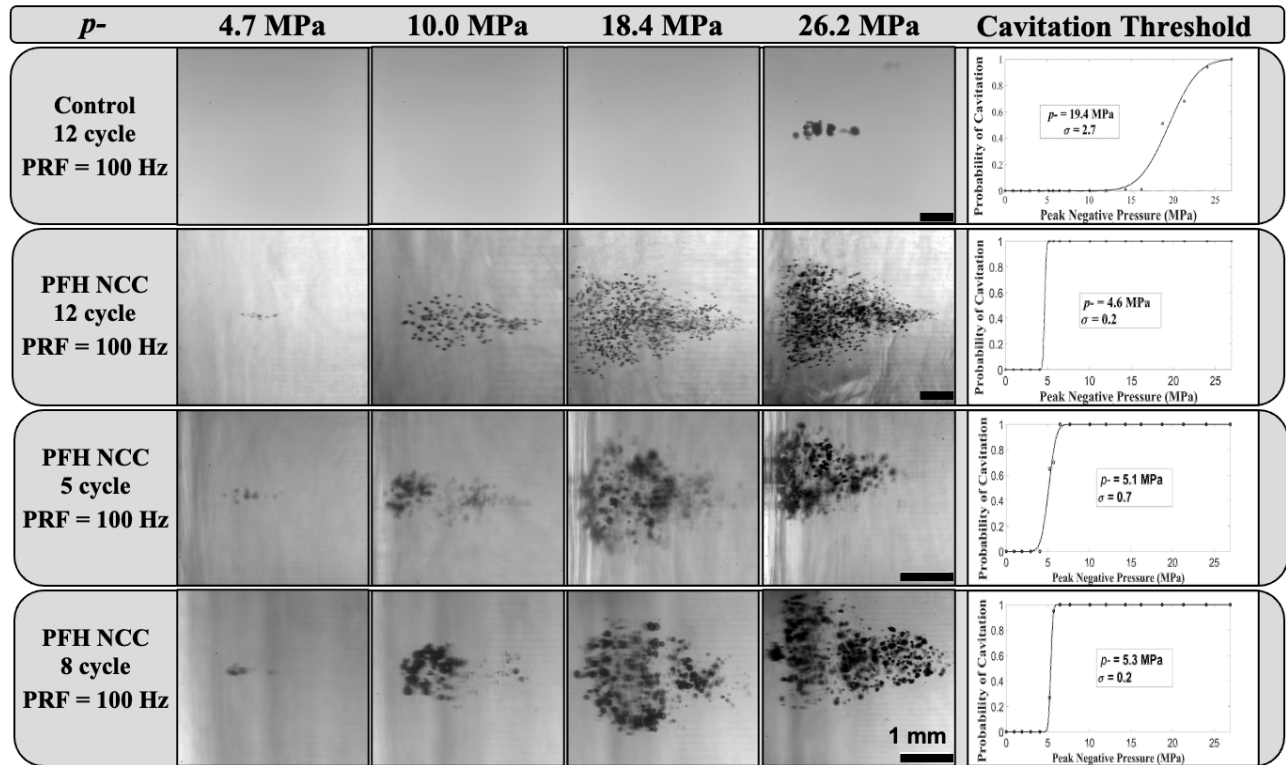


Figure 3-4. Images of cavitation bubble clouds for NCC gels under multi-cycle pulsing schemes at varying cycles using a 2 MHz transducer. Noticeably, for all trials the cavitation threshold was lowered a significant amount compared to the control. The dynamics of the bubble clouds are also visibly different, as expected with varying numbers of cycles. Cavitation threshold figures are also provided for each experiment.

3.4 Discussion: Multi-cycle Pulsing and NMH

As shown in **Figure 3-2**, visually it is observable that there are different dynamics at play compared to single-cycle pulsing. Visually, the bubble clouds are cavitating less dense and more peripheral bubbles are present compared to single-cycle pulsing while retaining the same cavitation threshold for NCCs. This notion could lead to investigations on significantly lowering treatment times for NMH while still producing consistent results. Larger tumors may be ideal candidates for this pulsing method due to the larger bubble clouds that can be generated at lower pressures using this technique. The cavitation threshold was decreased significantly for NCCs compared to single-cycle pulses and pulsing schemes at a lower PRF. This would enable smaller

and more portable devices to be used clinically due to the need of generating only a small pressure. This data should serve as the groundwork for future studies on NMH treatment times and viability with multi-cycle pulsing. The results found in this experiment are encouraging in the fact that they have shown the capability of NMH to achieve very low histotripsy cavitation thresholds which is something that has only recently begun to be explored. Having parameters for multi-cycle pulsing that are proven to induce cavitation at a desired threshold for NCCs can also lead to more rapid testing of NDs and NCCs at varying PFP and PFH concentrations. Recently, a study has been conducted using low-frequency, long-duration ultrasound pulses to induce NMH [64]. We plan to explore even longer pulses and new variations of cycle number and frequency parameters in future studies to more fully understand the cavitation nucleation and bubble cloud dynamics in NMH under the full range of potential treatment regimes.

3.5 Conclusions

This work investigated the ability of NCC to act as histotripsy cavitation agents with NMH for both single-cycle and multi-cycle pulsing schemes. The results of this study show the capability of NCCs to lower the histotripsy cavitation threshold to pressures significantly below the histotripsy intrinsic threshold. While previous studies have shown that this is possible with NMH, this study also shows the capability of these NCCs to further lower the cavitation threshold below previously recorded NMH pressures with the use of multi-cycle pulsing. Results demonstrated that while multi-cycle pulsing parameters lower the histotripsy cavitation threshold, altering the cycle number between 5, 8, and 12 cycles did not alter the threshold significantly. During the multi-cycle experiments, images were taken in between each pulse to determine if any stable bubbles were formed following ADV. These stable bubbles were not formed, as expected, following the existing literature of stable bubble formation not occurring

for particles on the nanoscale. Overall, this study demonstrates that artificial nuclei and multi-cycle parameters can offer a way to further reduce the histotripsy cavitation threshold significantly.

Chapter 4. Conclusions and Future Work

4.1 Conclusions

The experiments conducted in this thesis were designed to investigate histotripsy cavitation and acoustic droplet vaporization from PFH nanoparticles using single and multi-cycle pulsing modalities. The cavitation threshold of novel PFH NDs was investigated with single-cycle pulsing using a 500 kHz transducer in Chapter 2. Each of the NDs tested reduced the cavitation threshold from >28 MPa to a range of 20-25 MPa. Varying concentrations of PFH yielded different results in terms of cavitation threshold reduction. PEG500-F5, the ND that was tested both in gel and 1 mL liquid experiments showed no difference in threshold between the two. The 1 mL liquid experiments were conducted to ensure that the highest concentration of the ND was being tested. Chapter 3 presented the investigation of PFC and PFH NCCs using multi-cycle pulsing methods. There is no prior work published investigating NMH behavior with shock scattering histotripsy, and the results from this experiment matched our hypothesis that NMH could be effectively applied using this histotripsy pulsing regime. In all trials, the NCCs lowered the cavitation threshold to ranges lower than that of intrinsic threshold histotripsy. Stable bubble formation from ADV was not anticipated to occur with the NCCs due to their size, and this was confirmed upon investigation within only inertial cavitation characteristics of NMH observed for all experiments.

4.2 Future Directions

The ability of NMH to reduce cavitation threshold in multiple pulsing methods is the groundwork for future investigations. There are already active ongoing investigations alongside numerous published works on NMH with single-cycle and multi-cycle pulsing. The newly

synthesized NDs tested in the experiments for this thesis are unique in that their PFH concentrations are able to be determined upon synthesis. While the NDs reduced the cavitation threshold in each trial, these pressures did not align with the 10-15 MPa threshold of previously studied NMH works. There are currently ongoing studies looking to refine the concentration of NDs that have lowered the cavitation threshold to ~11 MPa for some samples. This notion indicates that future studies regarding the concentrations of the PFH content within the NDs should be conducted. As for multi-cycle pulsing, these experiments lay the groundwork for both NMH threshold studies using different parameters and ADV initiation with PFC NCCs. Multi-cycle pulsing as a whole has not been as thoroughly studied as intrinsic threshold histotripsy, which gives way to future work investigating the potential to develop more rapid pulsing schemes using this approach. The cavitation thresholds analyzed from these experiments are promising in that they are both consistent and effective at lowering the cavitation threshold. Testing NDs as well as different concentrations of PFC NCCs with multi-cycle pulsing in the future will only further characterize these nanoparticles as cavitation agents. There are also ongoing studies investigating the combination therapy aspect of the nanoparticles to reduce cavitation threshold as well as serve as drug delivery agents. ADV did not lead to the formation of stable bubbles during this experiment, though future studies can be conducted with a control particle that is similar in size or composition to that of the NCC to investigate the parameters and conditions required. Overall, NMH has been shown to be a viable treatment for multiple pulsing schemes with both the NDs and NCCs proving to be viable cavitation agents.

References

- [1] “Is Immunotherapy the Only Treatment Some People Need? - NCI,” Feb. 23, 2023. <https://www.cancer.gov/news-events/cancer-currents-blog/2023/neoadjuvant-immunotherapy-only-treatment> (accessed Apr. 04, 2023).
- [2] B. A. Chabner and T. G. Roberts, “Chemotherapy and the war on cancer,” *Nat. Rev. Cancer*, vol.

- 5, no. 1, Art. no. 1, Jan. 2005, doi: 10.1038/nrc1529.
- [3] D. Hanahan and R. A. Weinberg, “Hallmarks of cancer: the next generation,” *Cell*, vol. 144, no. 5, pp. 646–674, Mar. 2011, doi: 10.1016/j.cell.2011.02.013.
- [4] J. Zugazagoitia, C. Guedes, S. Ponce, I. Ferrer, S. Molina-Pinelo, and L. Paz-Ares, “Current Challenges in Cancer Treatment,” *Clin. Ther.*, vol. 38, no. 7, pp. 1551–1566, Jul. 2016, doi: 10.1016/j.clinthera.2016.03.026.
- [5] Y. Keisari, “Tumor abolition and antitumor immunostimulation by physico-chemical tumor ablation,” *Front. Biosci. Landmark Ed.*, vol. 22, no. 2, pp. 310–347, Jan. 2017, doi: 10.2741/4487.
- [6] J. A. Barreto, W. O’Malley, M. Kubeil, B. Graham, H. Stephan, and L. Spiccia, “Nanomaterials: Applications in Cancer Imaging and Therapy,” *Adv. Mater.*, vol. 23, no. 12, pp. H18–H40, 2011, doi: 10.1002/adma.201100140.
- [7] K. B. Bader, E. Vlaisavljevich, and A. D. Maxwell, “For Whom the Bubble Grows: Physical Principles of Bubble Nucleation and Dynamics in Histotripsy Ultrasound Therapy,” *Ultrasound Med. Biol.*, vol. 45, no. 5, pp. 1056–1080, May 2019, doi: 10.1016/j.ultrasmedbio.2018.10.035.
- [8] W. W. Roberts, “Development and Translation of Histotripsy: Current Status and Future Directions,” *Curr. Opin. Urol.*, vol. 24, no. 1, pp. 104–110, Jan. 2014, doi: 10.1097/MOU.0000000000000001.
- [9] Z. Izadifar, Z. Izadifar, D. Chapman, and P. Babyn, “An Introduction to High Intensity Focused Ultrasound: Systematic Review on Principles, Devices, and Clinical Applications,” *J. Clin. Med.*, vol. 9, no. 2, p. 460, Feb. 2020, doi: 10.3390/jcm9020460.
- [10] S. A. Curley, “Radiofrequency Ablation of Malignant Liver Tumors,” *Ann. Surg. Oncol.*, vol. 10, no. 4, pp. 338–347, May 2003, doi: 10.1245/ASO.2003.07.017.
- [11] “Full article: Treatment planning in microwave thermal ablation: clinical gaps and recent research advances.” <https://www.tandfonline.com/doi/full/10.1080/02656736.2016.1214883> (accessed Apr. 21, 2023).
- [12] K. D. Song, “Percutaneous cryoablation for hepatocellular carcinoma,” *Clin. Mol. Hepatol.*, vol. 22, no. 4, pp. 509–515, Dec. 2016, doi: 10.3350/cmh.2016.0079.
- [13] T. D. Khokhlova and J. H. Hwang, “HIFU for palliative treatment of pancreatic cancer,” *J. Gastrointest. Oncol.*, vol. 2, no. 3, pp. 175–184, Sep. 2011, doi: 10.3978/j.issn.2078-6891.2011.033.
- [14] D. S. K. Lu *et al.*, “Influence of Large Peritumoral Vessels on Outcome of Radiofrequency Ablation of Liver Tumors,” *J. Vasc. Interv. Radiol.*, vol. 14, no. 10, pp. 1267–1274, Oct. 2003, doi: 10.1097/01.RVI.0000092666.72261.6B.
- [15] L. Crocetti, T. de Baére, P. L. Pereira, and F. P. Tarantino, “CIRSE Standards of Practice on Thermal Ablation of Liver Tumours,” *Cardiovasc. Intervent. Radiol.*, vol. 43, no. 7, pp. 951–962, Jul. 2020, doi: 10.1007/s00270-020-02471-z.

- [16] S. Crouzet *et al.*, “Salvage high-intensity focused ultrasound (HIFU) for locally recurrent prostate cancer after failed radiation therapy: Multi-institutional analysis of 418 patients,” *BJU Int.*, vol. 119, no. 6, pp. 896–904, 2017, doi: 10.1111/bju.13766.
- [17] K. Pillai *et al.*, “Heat Sink Effect on Tumor Ablation Characteristics as Observed in Monopolar Radiofrequency, Bipolar Radiofrequency, and Microwave, Using Ex Vivo Calf Liver Model,” *Medicine (Baltimore)*, vol. 94, no. 9, p. e580, Mar. 2015, doi: 10.1097/MD.0000000000000580.
- [18] Z. Xu, T. L. Hall, E. Vlaisavljevich, and F. T. Lee, “Histotripsy: the first noninvasive, non-ionizing, non-thermal ablation technique based on ultrasound,” *Int. J. Hyperth. Off. J. Eur. Soc. Hyperthermic Oncol. North Am. Hyperth. Group*, vol. 38, no. 1, pp. 561–575, 2021, doi: 10.1080/02656736.2021.1905189.
- [19] M. Sadeghi-Goughari, S. Jeon, and H.-J. Kwon, “Enhancing Thermal Effect of Focused Ultrasound Therapy Using Gold Nanoparticles,” *IEEE Trans. NanoBioscience*, vol. 18, no. 4, pp. 661–668, Oct. 2019, doi: 10.1109/TNB.2019.2937327.
- [20] I. A. S. Elhelf, H. Albahar, U. Shah, A. Oto, E. Cressman, and M. Almekkawy, “High intensity focused ultrasound: The fundamentals, clinical applications and research trends,” *Diagn. Interv. Imaging*, vol. 99, no. 6, pp. 349–359, Jun. 2018, doi: 10.1016/j.diii.2018.03.001.
- [21] “First-in-man histotripsy of hepatic tumors: the THERESA trial, a feasibility study.” <https://www.tandfonline.com/doi/epdf/10.1080/02656736.2022.2112309?needAccess=true&role=button> (accessed Apr. 18, 2023).
- [22] HistoSonics, Inc., “The HistoSonics System for Treatment of Primary and Metastatic Liver Tumors Using Histotripsy (#HOPE4LIVER),” [clinicaltrials.gov](https://clinicaltrials.gov/ct2/show/NCT04573881), Clinical trial registration NCT04573881, Apr. 2023. Accessed: Apr. 20, 2023. [Online]. Available: <https://clinicaltrials.gov/ct2/show/NCT04573881>
- [23] C. Edsall, E. Ham, H. Holmes, T. L. Hall, and E. Vlaisavljevich, “Effects of frequency on bubble-cloud behavior and ablation efficiency in intrinsic threshold histotripsy,” *Phys. Med. Biol.*, vol. 66, no. 22, p. 225009, Nov. 2021, doi: 10.1088/1361-6560/ac33ed.
- [24] J. Khirallah *et al.*, “Nanoparticle-mediated histotripsy (NMH) using perfluorohexane ‘nanocones,’” *Phys. Med. Biol.*, vol. 64, no. 12, p. 125018, Jun. 2019, doi: 10.1088/1361-6560/ab207e.
- [25] M. Bacac and I. Stamenkovic, “Metastatic Cancer Cell,” *Annu. Rev. Pathol. Mech. Dis.*, vol. 3, no. 1, pp. 221–247, 2008, doi: 10.1146/annurev.pathmechdis.3.121806.151523.
- [26] E. Vlaisavljevich *et al.*, “Image-guided non-invasive ultrasound liver ablation using histotripsy: feasibility study in an in vivo porcine model,” *Ultrasound Med. Biol.*, vol. 39, no. 8, pp. 1398–1409, Aug. 2013, doi: 10.1016/j.ultrasmedbio.2013.02.005.
- [27] O. D. Kripfgans, J. B. Fowlkes, D. L. Miller, O. P. Eldevik, and P. L. Carson, “Acoustic droplet vaporization for therapeutic and diagnostic applications,” *Ultrasound Med. Biol.*, vol. 26, no. 7, pp. 1177–1189, Sep. 2000, doi: 10.1016/s0301-5629(00)00262-3.
- [28] S. Xu *et al.*, “Acoustic droplet vaporization and inertial cavitation thresholds and efficiencies of nanodroplets emulsions inside the focused region using a dual-frequency ring focused

- ultrasound,” *Ultrason. Sonochem.*, vol. 48, pp. 532–537, Nov. 2018, doi: 10.1016/j.ultsonch.2018.07.020.
- [29] C. Toydemir *et al.*, “Bioconjugated β -Cyclodextrin–Perfluorohexane Nanocone Clusters as Functional Nanoparticles for Nanoparticle-Mediated Histotripsy,” *Biomacromolecules*, vol. 23, no. 12, pp. 5297–5311, Dec. 2022, doi: 10.1021/acs.biomac.2c01110.
- [30] B. Kaymaz, W. Mustafa, S. Hall, E. Vlasisavljevich, O. Sensoy, and Y. Yuksel Durmaz, “Experimental and Computational Investigation of Clustering Behavior of Cyclodextrin–Perfluorocarbon Inclusion Complexes as Effective Histotripsy Agents,” *Mol. Pharm.*, vol. 19, no. 8, pp. 2907–2921, Aug. 2022, doi: 10.1021/acs.molpharmaceut.2c00268.
- [31] C. Edsall *et al.*, “Bubble Cloud Behavior and Ablation Capacity for Histotripsy Generated from Intrinsic or Artificial Cavitation Nuclei,” *Ultrasound Med. Biol.*, vol. 47, no. 3, pp. 620–639, Mar. 2021, doi: 10.1016/j.ultrasmedbio.2020.10.020.
- [32] Y.-J. Ho, Y.-C. Chang, and C.-K. Yeh, “Improving Nanoparticle Penetration in Tumors by Vascular Disruption with Acoustic Droplet Vaporization,” *Theranostics*, vol. 6, no. 3, pp. 392–403, 2016, doi: 10.7150/thno.13727.
- [33] M. L. Fabiilli, K. J. Haworth, N. H. Fakhri, O. D. Kripfgans, P. L. Carson, and J. B. Fowlkes, “The role of inertial cavitation in acoustic droplet vaporization,” *IEEE Trans. Ultrason. Ferroelectr. Freq. Control*, vol. 56, no. 5, pp. 1006–1017, May 2009, doi: 10.1109/TUFFC.2009.1132.
- [34] D. S. Li, O. D. Kripfgans, M. L. Fabiilli, J. B. Fowlkes, and J. L. Bull, “Initial nucleation site formation due to acoustic droplet vaporization,” *Appl. Phys. Lett.*, vol. 104, no. 6, p. 063703, Feb. 2014, doi: 10.1063/1.4864110.
- [35] E. Vlasisavljevich *et al.*, “Effects of Ultrasound Frequency and Tissue Stiffness on the Histotripsy Intrinsic Threshold for Cavitation,” *Ultrasound Med. Biol.*, vol. 41, no. 6, pp. 1651–1667, Jun. 2015, doi: 10.1016/j.ultrasmedbio.2015.01.028.
- [36] “Particle-Mediated Histotripsy for the Targeted Treatment of Intraluminal Biofilms in Catheter-Based Medical Devices | BME Frontiers.” <https://spj.science.org/doi/10.34133/2022/9826279> (accessed Apr. 19, 2023).
- [37] J. Wu, “The Enhanced Permeability and Retention (EPR) Effect: The Significance of the Concept and Methods to Enhance Its Application,” *J. Pers. Med.*, vol. 11, no. 8, p. 771, Aug. 2021, doi: 10.3390/jpm11080771.
- [38] M. Aliabouzar, K. N. Kumar, and K. Sarkar, “Effects of droplet size and perfluorocarbon boiling point on the frequency dependence of acoustic vaporization threshold,” *J. Acoust. Soc. Am.*, vol. 145, no. 2, p. 1105, Feb. 2019, doi: 10.1121/1.5091781.
- [39] S. Leporatti, “Thinking about Enhanced Permeability and Retention Effect (EPR),” *J. Pers. Med.*, vol. 12, no. 8, p. 1259, Jul. 2022, doi: 10.3390/jpm12081259.
- [40] “Tailoring nanoparticle designs to target cancer based on tumor pathophysiology.” <https://www.pnas.org/doi/10.1073/pnas.1521265113> (accessed Apr. 18, 2023).

- [41] J. C. Forster, W. M. Harriss-Phillips, M. J. Douglass, and E. Bezak, “A review of the development of tumor vasculature and its effects on the tumor microenvironment,” 2017, doi: 10.2147/HP.S133231.
- [42] N. Kaushal *et al.*, “Synergistic inhibition of aggressive breast cancer cell migration and invasion by cytoplasmic delivery of anti-RhoC silencing RNA and presentation of EPPT1 peptide on ‘smart’ particles,” *J. Controlled Release*, vol. 289, pp. 79–93, Nov. 2018, doi: 10.1016/j.jconrel.2018.07.042.
- [43] D. Pfister and M. Morbidelli, “Process for protein PEGylation,” *J. Controlled Release*, vol. 180, pp. 134–149, Apr. 2014, doi: 10.1016/j.jconrel.2014.02.002.
- [44] F. M. Veronese and G. Pasut, “PEGylation, successful approach to drug delivery,” *Drug Discov. Today*, vol. 10, no. 21, pp. 1451–1458, Nov. 2005, doi: 10.1016/S1359-6446(05)03575-0.
- [45] Y. Yuksel Durmaz, E. Vlaisavljevich, Z. Xu, and M. ElSayed, “Development of nanodroplets for histotripsy-mediated cell ablation,” *Mol. Pharm.*, vol. 11, no. 10, pp. 3684–3695, Oct. 2014, doi: 10.1021/mp500419w.
- [46] O. Aydin, E. Vlaisavljevich, Y. Yuksel Durmaz, Z. Xu, and M. E. H. ElSayed, “Noninvasive Ablation of Prostate Cancer Spheroids Using Acoustically-Activated Nanodroplets,” *Mol. Pharm.*, vol. 13, no. 12, pp. 4054–4065, Dec. 2016, doi: 10.1021/acs.molpharmaceut.6b00617.
- [47] Hall, Sarah, “Nanoparticle-mediated histotripsy for the treatment of breast cancer.” ISTU 2023 Lyon, Apr. 20, 2023.
- [48] A. D. Maxwell *et al.*, “Cavitation clouds created by shock scattering from bubbles during histotripsy,” *J. Acoust. Soc. Am.*, vol. 130, no. 4, pp. 1888–1898, Oct. 2011, doi: 10.1121/1.3625239.
- [49] K. B. Bader, M. J. Gruber, and C. K. Holland, “Shaken and Stirred: Mechanisms of Ultrasound-Enhanced Thrombolysis,” *Ultrasound Med. Biol.*, vol. 41, no. 1, pp. 187–196, Jan. 2015, doi: 10.1016/j.ultrasmedbio.2014.08.018.
- [50] E. Vlaisavljevich, A. Maxwell, M. Warnez, E. Johnsen, C. A. Cain, and Z. Xu, “Histotripsy-induced cavitation cloud initiation thresholds in tissues of different mechanical properties,” *IEEE Trans. Ultrason. Ferroelectr. Freq. Control*, vol. 61, no. 2, pp. 341–352, Feb. 2014, doi: 10.1109/TUFFC.2014.6722618.
- [51] M. Zhang *et al.*, “Initial Investigation of Acoustic Droplet Vaporization for Occlusion in Canine Kidney,” *Ultrasound Med. Biol.*, vol. 36, no. 10, pp. 1691–1703, Oct. 2010, doi: 10.1016/j.ultrasmedbio.2010.06.020.
- [52] K. Loskutova, D. Grishenkov, and M. Ghorbani, “Review on Acoustic Droplet Vaporization in Ultrasound Diagnostics and Therapeutics,” *BioMed Res. Int.*, vol. 2019, p. e9480193, Jul. 2019, doi: 10.1155/2019/9480193.
- [53] Z. Gao, A. M. Kennedy, D. A. Christensen, and N. Y. Rapoport, “Drug-loaded nano/microbubbles for combining ultrasonography and targeted chemotherapy,” *Ultrasonics*, vol. 48, no. 4, pp. 260–270, Aug. 2008, doi: 10.1016/j.ultras.2007.11.002.

- [54] P. S. Sheeran, S. Luois, P. A. Dayton, and T. O. Matsunaga, “Formulation and acoustic studies of a new phase-shift agent for diagnostic and therapeutic ultrasound,” *Langmuir ACS J. Surf. Colloids*, vol. 27, no. 17, pp. 10412–10420, Sep. 2011, doi: 10.1021/la2013705.
- [55] K. I. Kawabata, R. Asami, H. Yoshikawa, T. Azuma, and S. I. Umemura, “Sustaining microbubbles derived from phase change nanodroplet by low-amplitude ultrasound exposure,” *Jpn. J. Appl. Phys. Part 1 Regul. Pap. Short Notes*, vol. 49, no. 7 PART 2, Jul. 2010, doi: 10.1143/JJAP.49.07HF20.
- [56] T. U. Rehman, J. Khirallah, E. Demirel, J. Howell, E. Vlasisavljevich, and Y. Yuksel Durmaz, “Development of Acoustically Active Nanocones Using the Host–Guest Interaction as a New Histotripsy Agent,” *ACS Omega*, vol. 4, no. 2, pp. 4176–4184, Feb. 2019, doi: 10.1021/acsomega.8b02922.
- [57] E. Vlasisavljevich, Y. Y. Durmaz, A. Maxwell, M. ElSayed, and Z. Xu, “Nanodroplet-Mediated Histotripsy for Image-guided Targeted Ultrasound Cell Ablation,” *Theranostics*, vol. 3, no. 11, pp. 851–864, Oct. 2013, doi: 10.7150/thno.6717.
- [58] M. Oh-Ishi and T. Maeda, “Disease proteomics of high-molecular-mass proteins by two-dimensional gel electrophoresis with agarose gels in the first dimension (Agarose 2-DE),” *J. Chromatogr. B*, vol. 849, no. 1, pp. 211–222, Apr. 2007, doi: 10.1016/j.jchromb.2006.10.064.
- [59] A. D. Maxwell, C. A. Cain, T. L. Hall, J. B. Fowlkes, and Z. Xu, “Probability of cavitation for single ultrasound pulses applied to tissues and tissue-mimicking materials,” *Ultrasound Med. Biol.*, vol. 39, no. 3, pp. 449–465, Mar. 2013, doi: 10.1016/j.ultrasmedbio.2012.09.004.
- [60] E. Vlasisavljevich *et al.*, “Effects of Ultrasound Frequency on Nanodroplet-Mediated Histotripsy,” *Ultrasound Med. Biol.*, vol. 41, no. 8, pp. 2135–2147, Aug. 2015, doi: 10.1016/j.ultrasmedbio.2015.04.007.
- [61] E. Vlasisavljevich *et al.*, “The role of positive and negative pressure on cavitation nucleation in nanodroplet-mediated histotripsy,” *Phys. Med. Biol.*, vol. 61, no. 2, p. 663, Dec. 2015, doi: 10.1088/0031-9155/61/2/663.
- [62] M. Zhang *et al.*, “Acoustic Droplet Vaporization for Enhancement of Thermal Ablation by High Intensity Focused Ultrasound,” *Acad. Radiol.*, vol. 18, no. 9, pp. 1123–1132, Sep. 2011, doi: 10.1016/j.acra.2011.04.012.
- [63] Y. Li, T. L. Hall, Z. Xu, and C. A. Cain, “Enhanced Shock Scattering Histotripsy with Pseudo-Monopolar Ultrasound Pulses,” *IEEE Trans. Ultrason. Ferroelectr. Freq. Control*, vol. 66, no. 7, pp. 1185–1197, Jul. 2019, doi: 10.1109/TUFFC.2019.2911289.
- [64] B. Glickstein, M. Levron, S. Shitrit, R. Aronovich, Y. Feng, and T. Ilovitsh, “Nanodroplet-Mediated Low-Energy Mechanical Ultrasound Surgery,” *Ultrasound Med. Biol.*, vol. 48, no. 7, pp. 1229–1239, Jul. 2022, doi: 10.1016/j.ultrasmedbio.2022.02.018.